Diquark resonance and single top production at the Large Hadron Collider

Durmus Karabacak, S. Nandi, and Santosh Kumar Rai

Diquark resonance and single top production at the Large Hadron Collider

Durmus Karabacak[1], S. Nandi[2] and Santosh Kumar Rai[3]

Department of Physics and Oklahoma Center for High Energy Physics,

Oklahoma State University, Stillwater, OK 74078, USA

Abstract

New physics at the TeV scale is highly anticipated at the LHC. New particles with color, if within the LHC energy reach, will be copiously produced. One such particle is a diquark, having the quantum numbers of two quarks, and can be either a scalar or a vector. It will decay to two light quarks, or two top quarks, or a top and a light quark, (up or down type depending on the quantum number of the produced diquark). If singly produced, it can be looked for as a dijet resonance, or as giving extra contribution to the single top production or tt production. In this work, we consider a color sextet vector diquark having the quantum number of (ud) type, its resonance production , and the subsequent decay to tb, giving rise to excess contribution to the single top production. Even though the diquark mass is large, its strong resonance production dominate the weak production of tb for a wide range of the diquark mass. Also its subsequent decay to tb produce a very hard b-jet compared to the usual electroweak production. In addition, the missing energy in the final state event is much larger from the massive diquark decays. Thus, with suitable cuts, the final state with $b, \bar{b}$ and a charged lepton together with large missing energy stands out compared to the Standard Model background. We make a detailed study of both the signal and the background. We find that such a diquark is accessible at the 7 TeV LHC upto a mass of about 3.3 TeV with the luminosity 1 fb^{-1}, while the reach goes up to about 4.3 TeV with a luminosity of 10 fb^{-1}.

---

[1]Email address: durmas@ostatemail.okstate.edu

[2]Email address: s.nandi@okstate.edu

[3]Email address: santosh.rai@okstate.edu

1 Introduction

After more than one year of successful running of the Large Hadron Collider (LHC) at CERN, the data released by the two experiments, ATLAS and CMS, have not only improved on some of the limits set by the Tevatron experiments, but has already started giving some insights into the TeV scale. So far the results have proved to be consistent with predictions from the Standard Model (SM) with not much deviation which means that the LHC data is already pushing the energy frontier of any Beyond Standard Model (BSM) physics predictions. As expected the LHC data will be most sensitive to the strongly interacting sector with strong limits obtained from resonant searches of new physics exchanged in the s-channel. As the initial states at hadron colliders are colored particles, the most dominant contributions would be through new colored resonances as their couplings will be typically of the order of α_s. Such colored particles are predicted in many class of BSM theories such as " squarks" in R-Parity violating supersymmetric theories [1], "diquarks" in super-string inspired E_6 grand unification models [2] and "excited quarks" in composite models [3–6]. Some other possibilities include models with color-sextet fermions [7,8], color-octet vectors like axigluons [7,9] and colorons [10–13], models with color-triplet [14], color-sextet [15–17] or color-octet scalars [18,19].

These resonant states will decay to two light jets leading to modification of the dijet differential cross-section at large invariant mass. Both ATLAS and CMS collaborations have looked at the dijet signal and already put strong constraints on such resonances [20–23]. The most current bounds reported by the ATLAS experiment with data corresponding to 1.0 fb^{-1} integrated luminosity at 95% C.L. are 2.99 TeV for excited quarks, 3.32 TeV for axigluons and 1.92 TeV for color-octet scalars [22] while the CMS collaboration with the same amount of data reports lower bounds of 3.52 TeV for the E_6 diquarks , 2.49 TeV for the excited quarks, 2.47 TeV for the axigluons and colorons. [23].

We note that another interesting prospect other than the dijet signal at LHC will be the modifications to the top quark signal due to exchanges from such colored particles. We are interested in particular with particles of the diquark type which carry non-zero baryon number and couple to a pair of quarks or anti-quarks. A lot of studies exist in the literature for such diquarks and their resonant effects in the dijet signals [24–31] and pair production of top quarks [32–35] at the LHC. Scalar triplet diquark contributions have been previously considered in single top quark production at the LHC [36]. We focus on the case of vector *diquarks* which are

sextets of $SU(3)_C$ with charge $Q_e = \frac{1}{3}$. Such particles will be copiously produced as s-channel resonances and thus contribute to the dijet final state. It is worth noting that these diquarks will also contribute to the single top quark production leading to significant enhancement in the production cross-section for the process which is the main thrust of this work. An important property of the top, in contrast to lighter quarks, is that it decays before hadronization and thus the single top quark production at the LHC can prove to be an ideal channel to probe for new physics.

For our study of the vector diquark we follow the formalism presented in Ref [29]. In Sec. 2 we present the formalism and give the basic interaction Lagrangian relevant for our study and in Sec. 3 we discuss the single top production cross-section at the LHC and give our results for the signal coming from the diquark exchange and present a detail analysis by comparing the signal with the SM background for the single top channel. In Sec. 4 we discuss the LHC reach for diquark contribution in the single top channel and in Sec. 5 we give our conclusions with future outlook.

2 Formalism

We are interested in new elementary particles that couple to a pair of quarks directly which would imply that they carry exotic baryon number. As the LHC is a proton-proton machine, the initial states comprised of the the valence quarks will lead to enhanced flux in the parton distributions for the collision between a pair of valence quarks such as uu, dd or ud. Any new particle that couples to these pairs would carry a baryon number $B = \dfrac{2}{3}$ and will be charged under the SM color gauge group $SU(3)_C$. Such states are generally referred to as "diquarks". We follow the formalism presented in Ref [29] where the states are classified according to their charges under the SM gauge group $SU(3)_C \times SU(2)_L \times U(1)_Y$ and their spin (J) given by

$$(SU_3, SU_2)_{Q_e}^J, \tag{2.1}$$

where Q_e indicates the electric charge $(T_3 + Y)$. The colored exotics (diquarks) that couple to the valence quark pairs can be either color anti-triplets or sextets. Writing them in the notation given by Eq. 2.1, we have

$$\Phi \sim (\mathbf{3} \oplus \bar{\mathbf{6}}, \mathbf{3})_{-4/3, 2/3, -1/3}^0, \quad \Phi_q \sim (\mathbf{3} \oplus \bar{\mathbf{6}}, \mathbf{1})_q^0 \ \ (q = -1/3, \ 2/3, \ -4/3),$$

$$A_U^\mu \sim (\mathbf{3} \oplus \bar{\mathbf{6}}, \mathbf{2})_{-1/3, -4/3}^1 \quad A_D^\mu \sim (\mathbf{3} \oplus \bar{\mathbf{6}}, \mathbf{2})_{2/3, -1/3}^1, \tag{2.2}$$

plus their charge conjugates. The gauge invariant Lagrangian describing the interaction of the above states is given by [29]

$$
\begin{aligned}
\mathcal{L}_{qqD} \quad \sim \quad & K_{ab}^{j} \left[y_{\alpha\beta} \, \overline{Q_{\alpha a}^{C}} i\sigma_2 \Phi^j Q_{\beta b} + \kappa_{\alpha\beta} \, \Phi_{-1/3}^{j} \overline{Q_{\alpha a}^{C}} i\sigma_2 Q_{\beta b} \right. \\
& + \lambda_{\alpha\beta}^{1/3} \, \Phi_{-1/3}^{j} \overline{D_{\alpha a}^{C}} U_{\beta b} + \lambda_{\alpha\beta}^{2/3} \, \Phi_{2/3}^{j} \overline{D_{\alpha a}^{C}} D_{\beta b} + \lambda_{\alpha\beta}^{4/3} \, \Phi_{-4/3}^{j} \overline{U_{\alpha a}^{C}} U_{\beta b} \\
& \left. + \lambda_{\alpha\beta}^{U} \, \overline{Q_{\alpha a}^{C}} i\sigma_2 \gamma_\mu A_U^{j\,\mu} U_{\beta b} + \lambda_{\alpha\beta}^{D} \, \overline{Q_{\alpha a}^{C}} i\sigma_2 \gamma_\mu A_D^{j\,\mu} D_{\beta b} \right] + \text{h.c.}, \quad (2.3)
\end{aligned}
$$

where $\Phi^j = \frac{1}{2}\sigma_\ell \Phi_\ell^j$. The σ_ℓ are the usual $SU(2)_L$ Pauli matrices while K_{ab}^{j} represent the $SU(3)_C$ Clebsch-Gordan coefficients with the quark color indices $a, b = 1, 2, 3$. The color index for the diquark fields are denoted as $j = 1 - N_D$ where N_D is the dimension of the triplet $(N_D = 3)$ or antisextet $(N_D = 6)$ representation. The coefficient K_{ab}^{j} is antisymmetric (symmetric) under the color indices ab for the $\bar{\mathbf{3}}$ $(\mathbf{6})$ representation. C denotes charge conjugation while α, β represent the fermion generation indices.

The states given in Eq. (2.2) will mix after electroweak symmetry breaking occurs and one can rewrite the physical states according to their SU_3 color quantum number $(\mathbf{3}, \bar{\mathbf{6}})$ and electric charges $(-4/3, \, 2/3, \, -1/3)$. We are only interested in the couplings of the vector diquark and thus keep only terms that involve the vector fields which we denote as $V_{2U}^{N_D}, V_{U}^{N_D}, V_{D}^{N_D}$, where the subscripts $2U, U$, and D in the fields indicates their electric charge $|Q|$ of two up type quarks, one up and one down type quark respectively. The relevant interactions among the physical vector states (diquarks) are then described by the following effective Lagrangian density

$$
\mathcal{L}_{qqD}^{V} = K_{ab}^{j} \left[\lambda_{\alpha\beta}^{\prime 2U} V_{2U}^{j\mu} \overline{u^c}_{\alpha a} \gamma_\mu P_R u_{\beta b} + \lambda_{\alpha\beta}^{\prime U} V_{U}^{j\mu} \overline{d^c}_{\alpha a} \gamma_\mu P_R d_{\beta b} + \lambda_{\alpha\beta}^{\prime D} V_{D}^{j\mu} \overline{u^c}_{\alpha a} \gamma_\mu P_\tau d_{\beta b} \right] + \text{h.c.} \quad (2.4)
$$

where $P_\tau = \frac{1}{2}(1 \pm \gamma_5)$ with $\tau = L, R$ representing left and right chirality projection operators and superscript μ is the Lorentz four vector index. Note that we have suppressed the dimension index (N_D) which is common to all the states as the interaction for the triplet and antisextet are similar. The more general form of the Lagrangian can be found in Ref [29].

The coupling λ's involved in Eq. 2.4 are completely arbitrary and can be large as long as they remain perturbative $\left(\frac{\lambda^{\prime 2}}{4\pi} < 1 \right)$. However most of them are tightly constrained by flavor physics. In our case we find that the more stringent constraints come from collider data such as the Tevatron and LHC. We focus on the contribution coming from the interaction vertex that involve the vector diquark V_D^μ which will mediate the production of top quark at the LHC and modify the event rates for single top quark production. The diquarks can couple to the initial state valence partons in the proton and are only constrained by their coupling strengths. Thus

they will contribute to the dijet production at the LHC which is enhanced for lighter mass and will be possible to study through the invariant mass distribution in the dijet channel. Both the CMS [23] and ATLAS [22] experiments at LHC have looked for such narrow resonances in the dijet channel and effectively lead to strong constraints on such massive resonances. For our study we have restricted ourselves to couplings of type λ_{ii} only. We note that couplings of type λ_{ij}, where $i \neq j$ could also give rise to single top production, but we assume them to be too small to make any significant contribution and are therefore neglected and play no role in our analysis. It is worth noting that these colored states do not have direct coupling to a pair of gluons and thus the production cross section for such particles is limited by the flux of the initial partons in the proton at the LHC.

3   Single top production at the LHC

We study the single top-quark production at the LHC where the new physics effects on the single top production come from the exchange of the vector diquark (V_D) in the s-channel. The single top production in the SM can proceed in three different channels as shown in Fig. 1. We
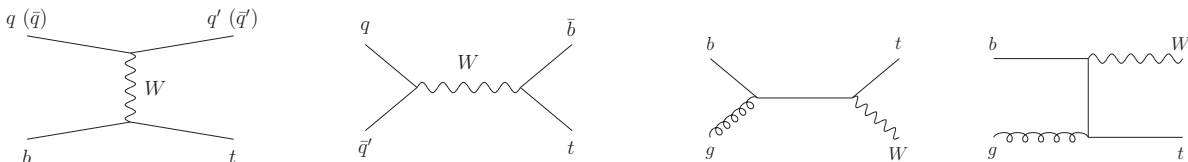

Figure 1: The leading order (LO) Feynman diagrams for the t-channel, s-channel, and tW production mode for the single top at hadron colliders.

can have the (a) t-channel production of the top quark with a light quark in the final state, (b) s-channel mode where the top quark is produced with $\bar{b}$-quark via exchange of a W-boson and (c) the associated production of the top quark with the W-boson via initial state gluon-bottom fusion. The t-channel processes, $qb \to q't$ and $\bar{q}b \to \bar{q}'t$, are significantly larger than the s-channel processes, $q\bar{q}' \to \bar{b}t$ at LHC. The associated production of a top quark with a W boson, $bg \to tW^-$, has a smaller cross-section compared to the t-channel processes, but is significantly larger than the s-channel processes. The approximate theoretical cross-sections for the 7 TeV LHC for the single top processes calculated at NLO with next-to-next-to-leading-logarithm (NNLL) corrections [37–39] are shown in Table 1.

Channel	NLO+NNLL cross-section (pb)
t-channel top	$41.7^{+1.6}_{-0.2} \pm 0.8$
t-channel anti-top	$22.5 \pm 0.5^{+0.7}_{-0.9}$
s-channel top	$3.17 \pm 0.06^{+0.13}_{-0.10}$
s-channel anti-top	$1.42 \pm 0.01^{+0.06}_{-0.07}$
tW^-	$7.8 \pm 0.2^{+0.5}_{-0.6}$

Table 1: The NLO+NNLL cross-sections for single top (anti-top) production of mass $m_t = 173$ GeV at the LHC with 7 TeV center-of-mass energy. Note that the cross section for $\bar{t}W^+$ production is identical to that for tW^-

.

For our purposes, we are interested in the corrections to the s-channel production mode for the single top through the vector diquark exchange. The Feynman diagram contributing to the production mode is shown in Fig. 2. Note that the final state has a b-quark instead of
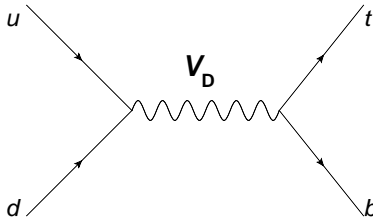

Figure 2: Feynman diagram for the s-channel contribution of the vector diquark for the single top production at LHC.

the $\bar{b}$ unlike the s-channel mode in SM. The anti-top production through the charge-conjugated vertices would be significantly suppressed and different because of the small flux of the anti-partons in the colliding protons. Although the top and anti-top production can be distinguished through the charged lepton identification coming from the decay, it is practically impossible to distinguish the b from the $\bar{b}$ at LHC. Thus we focus only on the production mode $pp \to tb$ which will show an effective increase in the s-channel single top production. As the final state distinctly differs from the SM subprocess, there are no interference term contributions. Thus we can simply evaluate the new physics contributions by calculating the subprocess $ud \to V_D^* \to tb$ at LHC and convolute it with the appropriate parton density functions (PDF) for the initial colliding partons.
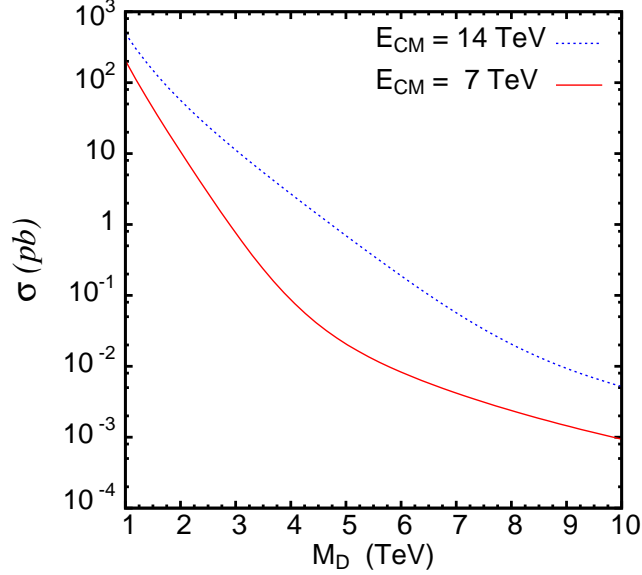
Figure 3: *The production cross-section for* $pp \rightarrow tb + X$ *at LHC as a function of the diquark mass* M_D *for two values of the center-of-mass energy,* $E_{CM} = 7$ *and* 14 *TeV. Note that we have chosen* $\lambda'_{\alpha\alpha} = 1$ *and* $Q = m_t$, *the mass of the top-quark.*

The amplitude for the subprocess $ud \rightarrow V_D^* \rightarrow tb$ using the interaction vertices from the Lagrangian as given by Eq. 2.4 is

$$\overline{|\mathcal{M}|}^2 = \frac{\lambda'^2_{11} \lambda'^2_{33}}{[(\hat{s} - M_D^2)^2 + M_D^2 \Gamma_D^2]} [(\hat{s} - m_t^2)(1 + \cos\theta)][\hat{s} + m_t^2 + (\hat{s} - m_t^2)\cos\theta] \qquad (3.5)$$

where θ is the scattering angle of the top-quark with the beam axis, M_D is the mass of the vector diquark with a decay width of Γ_D, λ's are the Yukawa couplings, m_t is the top quark mass and $\hat{s} = x_1 x_2 s$ is the effective center-of-mass energy squared for the colliding partons carrying x_i fraction of proton energy. The parton-level Born cross-section then reads

$$\hat{\sigma}(ud \rightarrow tb) = \frac{1}{48\pi \hat{s}^2} \frac{\lambda'^2_{11} \lambda'^2_{33}}{[(\hat{s} - M_D^2)^2 + M_D^2 \Gamma_D^2]} (\hat{s} - m_t^2)^2 (m_t^2 + 2\hat{s}) \qquad (3.6)$$

The total production cross-section at the LHC for the subprocess through the vector diquark exchange in the s-channel is given by

$$\sigma(pp \rightarrow tb + X) = \sum_{i=1}^{2} \int dx_1 \int dx_2 \, \mathcal{F}_{u_i}(x_1, Q^2) \times \mathcal{F}_{d_i}(x_2, Q^2) \times \hat{\sigma}(u_i d_i \rightarrow tb) \qquad (3.7)$$

where $\mathcal{F}_{u_i}$ and $\mathcal{F}_{d_i}$ denote the PDF's for the up-type and down-type quarks in the colliding protons, while Q is the factorization scale. We plot the leading-order production cross section

for the process $pp \to tb + X$ at LHC for the center-of-mass energies of 7 TeV and 14 TeV as a function of the diquark mass in Fig. 3. We have set the factorization scale $Q = m_t$ and used the `CTEQ6l1` parton density functions [40]. We have used $\lambda'_{\alpha\alpha} = 1$ for evaluating the production cross-section in Fig. 3. Note that for the diquark mass $M_D < 4$ TeV the contribution is more than 0.1 pb at the current LHC center-of-mass energy for order $\lambda' = 1$ couplings. However the couplings are severely constrained for the first two generations from the dijet data at the LHC and thus effective cross-sections would be actually smaller for the low values of diquark mass. For the diquarks of mass greater than 1 TeV we can assume the top quark as massless and in this limit the total decay width V_D (for decays to $ud + cs + tu$) is given as

$$\Gamma_D = \frac{\lambda'^2 M_D}{8\pi}. \tag{3.8}$$

As the diquark exchange in the s-channel would contribute to the dijet cross-section there are strong constraints on its mass and coupling strength [22,23] . For order one coupling the current bound is 3.52 TeV for the E_6 diquarks. However, we must note that the coupling strength of the diquark to the third generation λ'_{33} is unconstrained by the dijet data and thus the direct bounds on the diquark mass can be relaxed for smaller values of the couplings. The λ'_{33} coupling is however constrained from the upper bound on the single-top cross-section in the s-channel which is < 26.5 pb at 95% C.L. using a cut-based analysis [41]. For our analysis, we have assumed that the couplings to all generations are the same and thus we use the constraints given by the upper bound on the cross-section times branching ratio $(\sigma \times B)$ on the dijet rate [23] to evaluate the cross-sections for different values of the diquark mass.

As pointed out before, we would like to see the effect of the diquark contributions to the s-channel production of single top-quark. To analyze this we focus on the semileptonic decay mode of the produced top quark leading to the following final state:

$$pp \longrightarrow (t \to bW^+)b \longrightarrow (W^+ \to \ell^+ \nu_\ell)bb \longrightarrow \ell^+ bb \not{E}_T \tag{3.9}$$

where we restrict ourselves to the choice of $\ell = e, \mu$ for the charged lepton. As it is very difficult to differentiate between a b and $\bar{b}$ even with the heavy flavor tagging of the jets in the final state, we are looking at a final state with one positively charged lepton (ℓ^+) and two hard b-jets and missing transverse momenta. A similar final state is expected in the SM from the s-channel single top production as well as various other subprocesses which can lead to similar final state topology. At the LHC the significant contributions in the SM to this final state come from the

following processes:

$$p\ p \longrightarrow \qquad W^+Z,\ \ t\bar{t},\ \ t\bar{b},\ \ W^+b\bar{b}$$

$$\hookrightarrow \qquad tj,\ \ W^+jj,\ \ (tW^- + \bar{t}W^+),\ \ W^+W^- \qquad (3.10)$$

where the processes in the upper row of Eq. 3.10 give two b-jets while the processes in the lower row lead to light quarks in the final state which are identified as b-jets because of mistag. For our parton-level analysis, we choose a b-tagging efficiency of 50% while the mistag rate for light quarks tagged as b-jets is taken as 1%. We must point out that the b-tag efficiency and the mistag rates are dependent on the transverse momenta (p_T) and rapidity (η). Our choice does not include these effects. However, to do such detailed analysis one would also need to include various other systematics including showering and hadronization effects at the LHC and detector-level simulations which is beyond the scope of this work. So we assume that our choice for the efficiencies and the mistag rate is a good approximation when averaged over the entire range of transverse momenta for the quarks within the allowed rapidity gap.

To select the particles in the final state we demand that they satisfy some basic kinematic selection cuts.

- For the two b-jets we demand that they have a minimum transverse momenta given by $p_T^b > 20$ GeV and are within the rapidity gap $|\eta_b| < 2.5$.

- The charged lepton ($\ell^+ = e^+, \mu^+$) is required to have a minimum transverse momenta given by $p_T^{\ell^+} > 20$ GeV and is within the rapidity gap $|\eta_{\ell^+}| < 2.5$.

- The final states must account for a minimum missing transverse momenta given by $\not{E}_T > 50$ GeV.

- To resolve the final states in the detector they should be well separated. To achieve this we require that they satisfy $\Delta R_{ij} > 0.2$ with i, j representing the b-jets and the charged lepton. The variable ΔR_{ij} defines the separation of two particles in the (η, ϕ) plane of the detector with $\Delta R_{ij} = \sqrt{(\eta_i - \eta_j)^2 + (\phi_i - \phi_j)^2}$, where η and ϕ represent the pseudo-rapidity and azimuthal angle of the particles respectively.

- To suppress large contributions of gluon splitting into two (b) jets we demand that the minimum invariant mass of two b-jets satisfy $M_{b_1 b_2}^{inv} > 10$ GeV.

- We also demand that there are no additional jets with $p_T > 20$ GeV or additional charged leptons with $p_T > 10$ GeV.

With these basic selection cuts and efficiency rates for b-tagging we evaluate the contributions to the final state within the SM using the event generator MadGraph 5 [42]. The

Sub-process	$\sigma(\ell^+ + 2b + \not{E}_T)$ (fb)	$\sigma(\ell^+ + 2b + \not{E}_T)$ (fb) (after cut $p_T^{b_1} > 400$ GeV)
$pp \to WZ$	7.33	4.25×10^{-3}
$pp \to Wjj$	9.97	4.54×10^{-2}
$pp \to Wb\bar{b}$	87.55	0.25
$pp \to tW$	0.53	2.58×10^{-4}
$pp \to t\bar{t}$	5.51	1.9×10^{-3}
$pp \to tj$	6.24	2.65×10^{-3}
$pp \to t\bar{b}$	23.32	0.26
$pp \to V_D^* \to tb$	51.02 (4.73)	47.24 (4.55)

Table 2: Illustrating the leading-order (LO) parton-level SM background cross section for the dominant sub-processes contributing to the final state $\ell^+ + 2b + \not{E}_T$ and the signal for two values of diquark mass of $M_D = 2(3)$ TeV and coupling $\lambda'_{11}\lambda'_{33} = 0.45$ with basic selection cuts. Also shown is the cross section after an additional cut on the leading b-jet ($p_T > 400$ GeV) is imposed. Note that we have included a b-tagging efficiency of 50% for the b-jets and a mistag rate of 1% for the light quarks to be tagged as b-jets for the final cross sections shown in the table.

contributions from the different processes are collected in Table 2. We note that while the s-channel single top quark process gives a significant rate, the most dominant contribution comes from the QCD induced process $pp \to W^+ b\bar{b}$. We note that in Ref. [41] the $t\bar{t}$ contribution is shown to be significantly larger (albeit with large error bars) unlike our analysis. While we have made a leading-order parton-level analysis using MadGraph5, Ref. [41] has the full effects of a hadron collider environment, such as parton-showering effects, hadronization and fragmentation and also different stages of triggering on final states as well as detector level effects. Therefore a direct comparison of our analysis with that of Ref. [41] is not possible. We note that this mismatch can be possible when the jets fragment into softer jets and pass the veto

cuts leading to larger event rates for the $t\bar{t}$ which has the largest production cross section. Our parton-level analysis does not allow for such fragmentation effects and therefore leads to much smaller numbers following the jet veto cuts. Summing over all significant contributions we find that the LO SM cross-section at LHC with $\sqrt{s} = 7$ TeV, for the final state of $\ell^+ + 2b + \not{E}_T$, is $\simeq 141$ fb.

We calculate the contributions for the above final state coming from the single top production via the exchange of a vector diquark in the s-channel for two different values of the diquark mass, viz. $M_D = 2$ TeV and $M_D = 3$ TeV. The effective couplings (assuming equal couplings to all generations) for the two choices of the diquark mass are restricted by the dijet data and given by the upper bound on $\sigma \times B(pp \to qq) < 0.121$ pb for $M_D = 2$ TeV and $\sigma \times B(pp \to qq) < 0.021$ pb for $M_D = 3$ TeV which lead to the upper bound on the effective λ' coupling as 0.24 and 0.3 respectively. Using the maximum allowed couplings, we estimate the cross-section $\sigma(\ell^+ + 2b + \not{E}_T)$ with the selection cuts and efficiency rates as 2.95 fb for $M_D = 2$ TeV and 0.42 fb for $M_D = 3$ TeV. However, we must note that these upper bounds are relaxed as there are no severe constraints on the diquark coupling to the third generation quarks. The dominant constraint comes from the upper bound of the s-channel single top-quark produc-
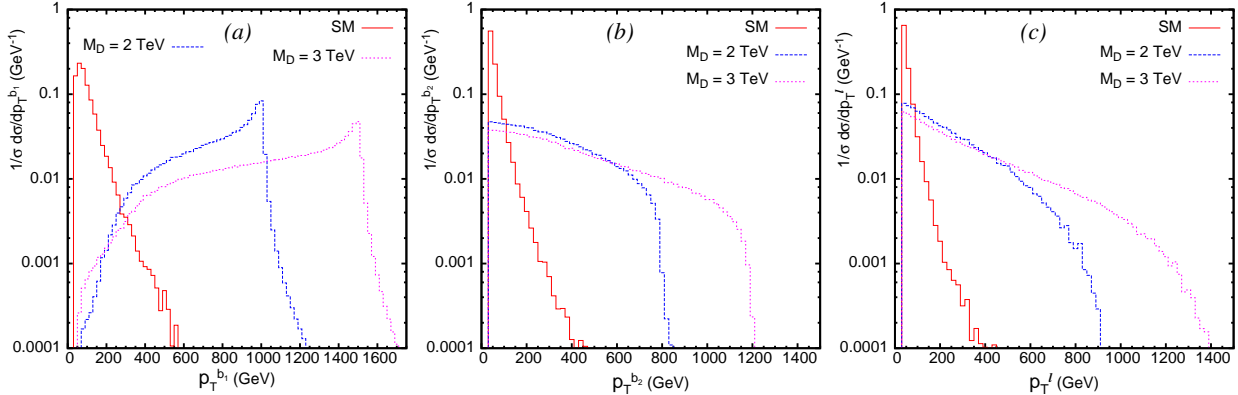

Figure 4: *Normalized differential distribution of the cross section as a function of the transverse momenta (p_T) of the visible particles in the final state for the SM background and the signal for two different values of the mass of the diquark $M_D = 2$ TeV and $M_D = 3$ TeV.*

tion cross-section at LHC [41] which puts an upper bound on the product of the couplings as $\lambda'_{ii}\lambda'_{33} \leq 0.45$. This allows the $\lambda'_{33} \simeq 1$ which would imply that the 2 TeV and 3 TeV diquark contributions to the $\ell^+ + 2b + \not{E}_T$ final state can be as large as 51 fb and 4.7 fb respectively. The relative significance of the diquark contributions can be enhanced by selecting events through

additional kinematic cuts suited to suppress the SM background without effecting the new physics signal. To understand the kinematic characteristics of the final state events coming from the SM processes and the diquark mediated process we plot the normalized differential distributions of the cross-section as a function of a few kinematical variables in Fig. 4-7.

In Fig. 4 we plot the normalized differential distribution of the cross-section with respect to the transverse momenta (p_T) of the visible particles in the final state, *viz.* the two b-jets and the charged lepton for the combined SM background and for the individual diquark contributions of mass $M_D = 2$ TeV and 3 TeV respectively. The b-jets are arranged according to their p_T's and so the leading b-jet (b_1) from the diquark mediated process comes almost always from the decay of the heavy diquark and thus peaks in the high p_T region when compared to the SM distribution which falls very rapidly as the b-jets get harder. As the diquark mass is increased we can see that the b-jet p_T peaks at much higher value (corresponding to the Jacobian peak at $\simeq \frac{M_D}{2}$). Again for the diquark mediated process the sub-leading b-jet (b_2) comes from the decay of a highly boosted top-quark and thus carries large p_T as shown in Fig. 4 (b). The charged lepton (ℓ^+) also shows similar behavior like the sub-leading b-jet as it also carries the boost of the top-quark from which it originates.
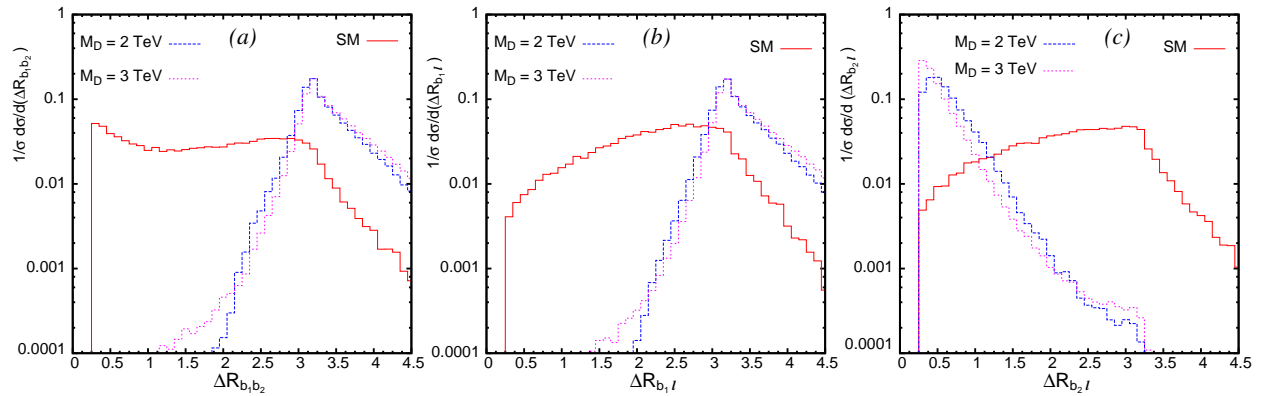

Figure 5: *Normalized differential distribution of the cross section as a function of the variable ΔR illustrating the isolation between two particles in the (η, ϕ) plane of the detector for the SM background and the signal for two different values of the mass of the diquark $M_D = 2$ TeV and $M_D = 3$ TeV.*

In Fig. 5 we plot the normalized differential distribution of the cross-section with respect to the isolation parameter ΔR between a pair of visible particles. Note that the characteristic behavior of particles coming from the decay of heavy resonance would be that they are produced

back-to-back in the transverse plane and are well separated which would imply peaking at large values of ΔR. This is the feature expected between the leading b-jet (b_1) and sub-leading b-jet (b_2) as well as the charged lepton (ℓ^+) when the events correspond to the process mediated by the diquark as evident in Fig. 5 (a) and (b). However, when the pair of particles originate from the decay of the highly-boosted top quark (b_2, ℓ^+) the relative separation between them would be much smaller as seen in the distributions shown in Fig. 5(c). The SM background does not have these characteristic features and shows a relatively uniform distribution in the ΔR variable because of contributions from multiple processes smoothening away any distinct effects of an individual contribution. It is worth noting that as the center of mass energy is increased the mother particles will have larger boost and will thus cause the decay products to be more collimated with smaller separation. Thus it is expected that stronger isolation cuts on the charged lepton and b-jet will reduce the event acceptance as the center of mass energy is increased.
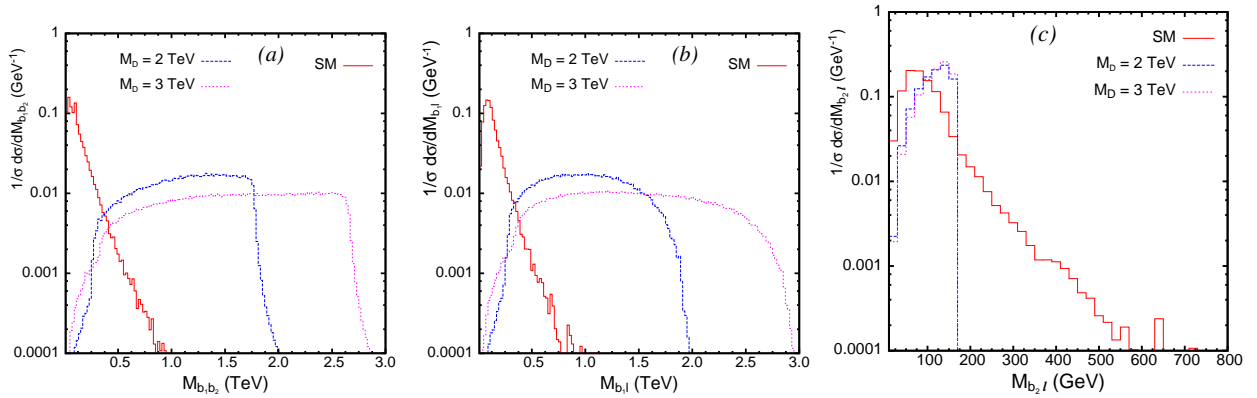

Figure 6: *Normalized differential distribution of the cross section as a function of the invariant mass of a pair of visible particles in the final state for the SM background and the signal for two different values of the mass of the diquark $M_D = 2$ TeV and $M_D = 3$ TeV.*

Another important kinematic variable relevant for any resonant production mode is the invariant mass of a pair of visible particles which reconstructs the mass of the resonant particle. In our case the heavy diquark decays to tb where the top decays further semileptonically. Thus we focus on the invariant mass distributions of the visible decay products. In Fig. 6 we plot the normalized differential distribution of the cross-section with respect to the invariant mass between a pair of visible particles. As shown in Fig. 6 (a) and (b), the distributions for the diquark mediated process for the invariant mass of the two b-jets ($b_1 b_2$) and the leading b-jet

with the charged lepton ($b_1\ell$) would peak for larger values and drop rapidly as it approaches the diquark mass which acts as an upper bound for the invariant mass value. The SM contributions however fall off very rapidly for large invariant mass in these particle pairs which is remnant of the fact that there are no heavy TeV mass particle in SM that can cause such a behavior. However, the invariant mass distribution for the sub-leading b-jet and the charged lepton has an upper cut-off at the top mass (m_t) for the diquark mediated process since the two particles almost always originate from the decay of the top quark and so the invariant mass of the decay products can never be greater than the mass of the mother particle. This can be seen in Fig. 6 (c). Note that the SM distribution has a long tail as there are other contributions which get superposed on the single top channel contribution making it significantly different from that of the diquark mode. We also note that the reconstructed invariant mass $M_{bb\ell\not{E}_T}$ will not only
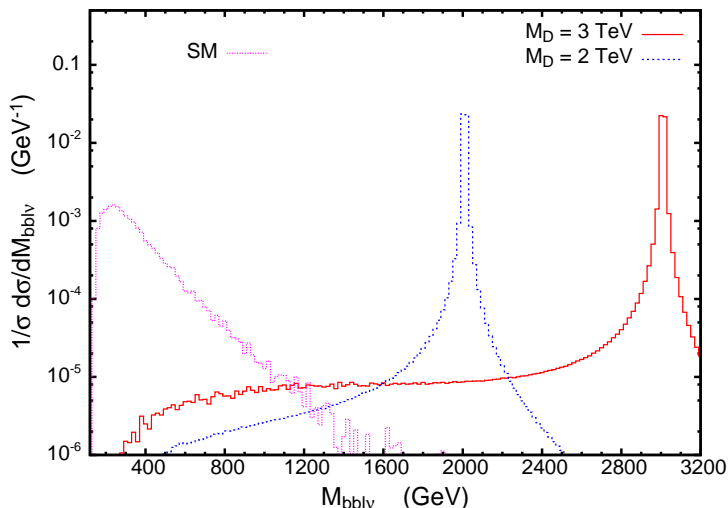

Figure 7: *Normalized differential distribution of the cross section as a function of the invariant mass of $b\bar{b}\ell^+\nu$ for the SM background and the signal for two different values of the mass of the diquark $M_D = 2$ TeV and $M_D = 3$ TeV.*

give us a good but approximate estimate of the diquark mass, but can also prove to be the most sensitive variable that discriminates the signal from the SM background. Using the W mass constraints one is able to reconstruct the p_z component of the neutrino and thus reconstruct the diquark mass through the invariant mass distribution of $b\bar{b}\ell\nu$ which we plot in Fig. 7 for the signal for two different mass of the diquark and the SM backround. As expected all the signal events are concentrated at M_D while the SM background trails off rapidly as $M_{bb\ell\not{E}_T} > 1$

TeV.

The dependence of the differential cross section on the different kinematic variables gives us a hint as to what should be the additional kinematic selection on the final state events which would make the diquark effects stand out against the SM contributions. As an effective cut on the invariant mass $M_{bb\ell\not{E}_T}$ will also rely on the knowledge of an unknown diquark mass, we find that the most effective alternative selection turns out to be the transverse momenta of the leading b-jet which originates from the decay of the diquark itself. We find that a more stringent requirement that the leading b-jet satisfies $p_T > 400$ GeV is very helpful in achieving a greater suppression of the SM background without affecting the diquark contributions significantly as shown in Table 2. With this additional cut, the SM background is reduced to $\simeq 0.59$ fb while the contribution for the diquark with mass $M_D = 2$ TeV is reduced only by 7% and that with mass $M_D = 3$ TeV is reduced only by 4%, thus significantly increasing the sensitivity to the diquark effects in the single top channel. The other promising variables are the ΔR and the invariant mass distribution of the two b-jets and that between the leading b-jet and the charged lepton which show significant difference between the diquark contribution and the SM background and will increase the signal significance with appropriate selection cuts when combined with the p_T selection.

4 LHC Sensitivity

We have simulated the events for diquark contribution and the SM background for the final state $\ell^+ + 2b + \not{E}_T$ at LHC with $\sqrt{s} = 7$ TeV for two values of the integrated luminosity of 1 fb^{-1} and 10 fb^{-1}. The statistical significance is calculated using [43]

$$\mathcal{S} = \sqrt{2 \times \left[(s+b)\ln(1+\frac{s}{b}) - s\right]} \tag{4.11}$$

where $s(b)$ is the number of diquark (SM background) events for the corresponding integrated luminosity. We show the sensitivity of the LHC to the diquark mass as a function of its coupling in Fig. 8. We have assumed that the vector diquark couples to all generations of SM quarks with the same strength such that $\alpha_\lambda \equiv \lambda_{ii}^{'2}/4\pi$. However α_λ in Fig. 8 can also be redefined as $\alpha_\lambda \equiv \lambda_{ii}^{'}\lambda_{33}^{'}/4\pi$ where $\lambda_{ii}^{'} = \lambda_{11}^{'} = \lambda_{22}^{'}$ which means that we can treat $\lambda_{33}^{'}$ which is unconstrained by dijet data separately. In Fig. 8 (a) we show the sensitivity of LHC in the (α_λ, M_D) parameter plane at 3σ statistical significance using the basic selection cuts
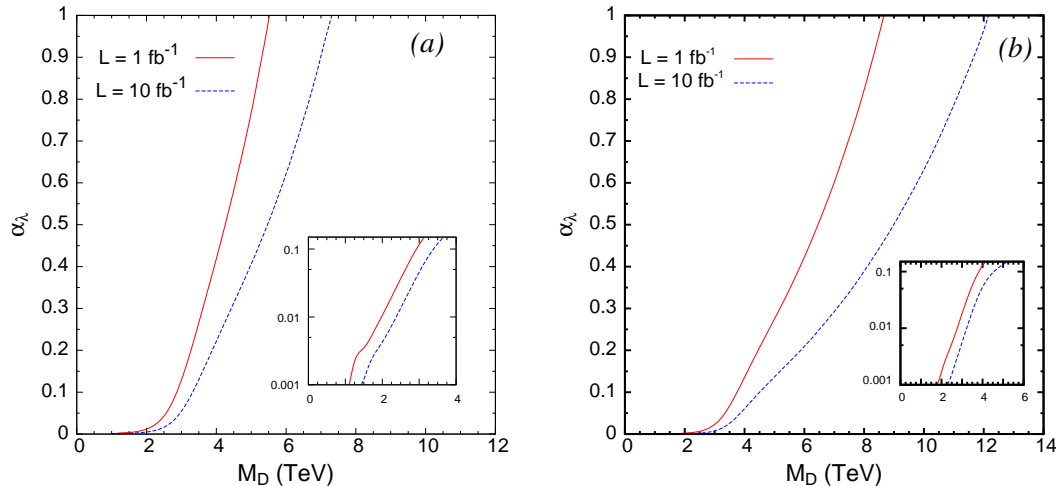
Figure 8: *Illustrating the reach for the LHC running at 7 TeV center-of-mass energy in the single top channel for the diquark mass and its coupling to SM quarks. The reach is shown for two values of the integrated luminosity where (a) shows the reach with the basic cuts used for the single top analysis while (b) shows the reach with a stronger cut of $p_T > 400$ GeV on the leading b-jet.*

discussed in Sec. 3. For $\lambda'^2 = 4\pi\alpha_\lambda \sim \mathcal{O}(1)$, we find that the LHC can rule out diquark of mass $M_D \simeq 2.8$ TeV with data corresponding to 1 fb^{-1} of integrated luminosity while the reach becomes $M_D \simeq 3.65$ TeV with data corresponding to 10 fb^{-1} with the same set of cuts. This reach is improved if we include the strong cut on the transverse momenta of the leading b-jet of $p_T > 400$ GeV, which we show in Fig. 8 (b). We find that with an integrated luminosity of 1 fb^{-1} which is already collected by each of the two experiments at LHC, the vector diquark mass accessible to LHC at 3σ statistical significance would be $M_D \simeq 3.25$ TeV while the reach expands to $M_D \simeq 4.3$ TeV with $L = 10$ fb^{-1}. We also note that the signal cross section is significantly enhanced when LHC runs at its full glory with the center of mass energy of 14 TeV (Fig. 3) thus leading to much more improved sensitivity and reach for larger values of the diquark mass. We estimate that using similar cuts and $p_T > 400$ GeV on the leading b-jet, LHC at $\sqrt{s} = 14$ TeV will be able to access a diquark mass of 5.5 TeV at 3σ statistical significance with and integrated luminosity of 1 fb^{-1}. We however must point out that our estimates are based on a leading-order parton level analysis and therefore cannot be expected to be exact. A more realistic estimate is possible with a complete simulation where the effects of the complex hadronic environment at LHC and detector level acceptance is included which

is beyond the scope of this work. We however expect that the essential kinematic features of the event characteristics will not be very different from what we have shown in our study. Thus we find that the single top channel with the appropriate cuts competes quite well with the dijet channel and can prove to be an improvement over the dijet channel if the coupling of the diquarks to the third generation quarks is larger than its coupling to the first two generations.

5 Summary and Conclusions

In this work we have studied the single top quark production at the LHC running at $\sqrt{s} = 7$ TeV. We have considered the effects of a vector diquark resonance on the single top quark production ($pp \to tb$) and compared it with the SM background for the $\ell^+ 2b \, \not{E}_T$ final state, where the top decays semileptonically. We find that there could be large enhancements in the single top quark production at LHC and find that various kinematic distributions effectively capture the essence of a heavy particle exchange which distinguish it from SM background. We have shown that the use of specific selection cuts on the kinematics of the final states can lead to improved significance for the effects of the diquark exchange and increase the LHC sensitivity to heavier diquark mass. We also note that for the vector diquark coupling more strongly to the third generation quarks than the first two generations, the LHC can be sensitive to higher values of the diquark mass when compared to the dijet channel.

In this work, we have restricted ourselves to the study of the sextet vector diquark exchange and we note that similar results can be also obtained for the triplet vector diquark or the scalar diquarks [36] which contribute to the single top quark production at the LHC. The vector diquark effects on the top quark polarization would be different from that of a scalar diquark exchange [34] as the Lorentz structure at the interaction vertices will be different which can prove to be a good discriminant in distinguishing the vector from the scalar exchange [44, 45].

Acknowledgments

References

[1] R. Barbier *et al.*, Phys. Rept. **420**, 1 (2005) [arXiv:hep-ph/0406039].

[2] J. L. Hewett and T. G. Rizzo, Phys. Rept. **183**, 193 (1989).

[3] A. De Rujula, L. Maiani and R. Petronzio, Phys. Lett. B **140**, 253 (1984).

[4] J. H. Kuhn and P. M. Zerwas, Phys. Lett. B **147**, 189 (1984).

[5] U. Baur, I. Hinchliffe and D. Zeppenfeld, Int. J. Mod. Phys. A **2**, 1285 (1987).

[6] U. Baur, M. Spira and P. M. Zerwas, Phys. Rev. D **42**, 815 (1990).

[7] P. H. Frampton and S. L. Glashow, Phys. Lett. B **190**, 157 (1987).

[8] S. P. Martin, Phys. Rev. D **46**, 2197 (1992) [arXiv:hep-ph/9204204].

[9] J. Bagger, C. Schmidt and S. King, Phys. Rev. D **37**, 1188 (1988).

[10] C. T. Hill, Phys. Lett. B **266**, 419 (1991).

[11] C. T. Hill and S. J. Parke, Phys. Rev. D **49**, 4454 (1994) [arXiv:hep-ph/9312324].

[12] D. A. Dicus, B. Dutta and S. Nandi, Phys. Rev, D51, 6085 (1995).

[13] D. A. Dicus, C. Kao and S. Nandi and J. Sayre, Phys. Rev. D83, 091702 (2011).
J. Sayre, D. A. Dicus, C. Kao and S. Nandi, Phys. Rev. D **84**, 015011 (2011)
[arXiv:1105.3219 [hep-ph]].

[14] K. S. Babu, R. N. Mohapatra and S. Nasri, Phys. Rev. Lett. **98**, 161301 (2007) [arXiv:hep-ph/0612357].

[15] J. C. Pati and A. Salam, Phys. Rev. D **10**, 275 (1974) [Erratum-ibid. D **11**, 703 (1975)].

[16] R. N. Mohapatra and R. E. Marshak, Phys. Rev. Lett. **44**, 1316 (1980) [Erratum-ibid. **44**, 1643 (1980)].

[17] Z. Chacko and R. N. Mohapatra, Phys. Rev. D **59**, 055004 (1999) [arXiv:hep-ph/9802388].

[18] B. A. Dobrescu, K. Kong and R. Mahbubani, Phys. Lett. B **670**, 119 (2008) [arXiv:0709.2378 [hep-ph]].

[19] C. T. Hill and E. H. Simmons, Phys. Rept. **381**, 235 (2003) [Erratum-ibid. **390**, 553 (2004)] [arXiv:hep-ph/0203079].

[20] G. Aad *et al.* [ATLAS Collaboration], Phys. Rev. Lett. **105**, 161801 (2010) [arXiv:1008.2461 [hep-ex]].

[21] V. Khachatryan *et al.* [CMS Collaboration], Phys. Rev. Lett. **105**, 211801 (2010) [arXiv:1010.0203 [hep-ex]].

[22] G. Aad *et al.* [ATLAS Collaboration], arXiv:1108.6311 [hep-ex].

[23] S. Chatrchyan *et al.* [CMS Collaboration], Phys. Lett. B **704**, 123 (2011) [arXiv:1107.4771 [hep-ex]].

[24] S. Atag, O. Cakir and S. Sultansoy, Phys. Rev. D **59**, 015008 (1999).

[25] E. Arik, O. Cakir, S. A. Cetin and S. Sultansoy, JHEP **0209**, 024 (2002) [arXiv:hep-ph/0109011].

[26] O. Cakir and M. Sahin, "Resonant production of diquarks at high energy pp, ep and e^+e^- Phys. Rev. D **72**, 115011 (2005) [arXiv:hep-ph/0508205].

[27] R. N. Mohapatra, N. Okada and H. B. Yu, Phys. Rev. D **77**, 011701 (2008) [arXiv:0709.1486 [hep-ph]].

[28] E. L. Berger, Q. H. Cao, C. R. Chen, G. Shaughnessy and H. Zhang, Phys. Rev. Lett. **105**, 181802 (2010) [arXiv:1005.2622 [hep-ph]].

[29] T. Han, I. Lewis and Z. Liu, JHEP **1012**, 085 (2010) [arXiv:1010.4309 [hep-ph]].

[30] G. F. Giudice, B. Gripaios and R. Sundrum, JHEP **1108**, 055 (2011) [arXiv:1105.3161 [hep-ph]].

[31] P. Richardson and D. Winn, arXiv:1108.6154 [hep-ph].

[32] V. Barger, T. Han and D. G. E. Walker, Phys. Rev. Lett. **100**, 031801 (2008) [arXiv:hep-ph/0612016].

[33] R. Frederix and F. Maltoni, JHEP **0901**, 047 (2009) [arXiv:0712.2355 [hep-ph]].

[34] H. Zhang, E. L. Berger, Q. H. Cao, C. R. Chen and G. Shaughnessy, Phys. Lett. B **696**, 68 (2011) [arXiv:1009.5379 [hep-ph]].

[35] N. Kosnik, I. Dorsner, J. Drobnak, S. Fajfer and J. F. Kamenik, arXiv:1111.0477 [hep-ph].

[36] I. Gogoladze, Y. Mimura, N. Okada and Q. Shafi, Phys. Lett. B **686**, 233 (2010) [arXiv:1001.5260 [hep-ph]].

[37] N. Kidonakis, Phys. Rev. D **83**, 091503 (2011) [arXiv:1103.2792 [hep-ph]].

[38] N. Kidonakis, Phys. Rev. D **81**, 054028 (2010) [arXiv:1001.5034 [hep-ph]].

[39] N. Kidonakis, Phys. Rev. D **82**, 054018 (2010) [arXiv:1005.4451 [hep-ph]].

[40] J. Pumplin, D. R. Stump, J. Huston, H. L. Lai, P. M. Nadolsky and W. K. Tung, JHEP **0207**, 012 (2002) [arXiv:hep-ph/0201195].

[41] ATLAS Collaboration, *Search for s-channel single top-quark production in pp collisions at $\sqrt{s} = 7$ TeV*, ATLAS-CONF-2011-118 (2011).

[42] J. Alwall, M. Herquet, F. Maltoni, O. Mattelaer and T. Stelzer, JHEP **1106**, 128 (2011) [arXiv:1106.0522 [hep-ph]].

[43] CMS Collaboration, G.L. Bayatian et. al., *CMS Physics: technical design report*, CERN-LHCC-2006-001.

[44] M. Arai, K. Huitu, S. K. Rai and K. Rao, JHEP **1008**, 082 (2010) [arXiv:1003.4708 [hep-ph]].

[45] K. Huitu, S. K. Rai, K. Rao, S. D. Rindani and P. Sharma, JHEP **1104**, 026 (2011) [arXiv:1012.0527 [hep-ph]].